Available online at www.sciencedirect.com

SCIENCE DIRECT®

ELSEVIER

Polymer 46 (2005) 6335–6346

polymer

www.elsevier.com/locate/polymer

Monitoring elasticity and orientation in syndiotactic polypropylene

Gautam Parthasarathy, Michael S. Sevegney, Rangaramanujam M. Kannan*

Department of Chemical Engineering and Material Science, Wayne State University, 1121 Engineering, 5050 Anthony Wayne Drive, Detroit, MI 48202, USA

Received 1 February 2005; received in revised form 13 May 2005; accepted 18 May 2005
Available online 1 July 2005

Abstract

The effect of temperature on the elasticity and structure of syndiotactic polypropylene (sPP) is investigated using a combination of WAXD and rheo-optical FTIR spectroscopy. sPP has a rich crystal structure, which leads to unique mechanical behavior. Beyond yield point, it exhibits elastic response associated with deformation-induced structure–structure transformation. The structure and orientation were measured both during and after uniaxial tensile stretching of films (up to 200%) as a function of temperature (25–70 °C). Our WAXD and rheo-FTIR results suggest that as the temperature increases, there is a reduction in the extent of helical to *trans*-planar conformational change upon stretching. When the strain is released, there is partial transformation of *trans*-planar conformation back to helical. The presence and orientation of the *trans*-planar conformation plays a key role on the elastic behavior of sPP beyond the yield point. Rheo-optical FTIR dichroism studies provide further insights into the elasticity in syndiotactic polypropylene. Different proportions of helical and *trans*-planar conformations orient to different extents. The helical conformation does not orient appreciably at higher temperature though they are present beyond the yield point. In contrast, the *trans*-planar chains show a significant increase in dichroism beyond the yield point, suggesting that there is a difference in mobility (orientation) of the helical and *trans*-planar chains. This further supports the importance of *trans*-planar chains on the elastic behavior.

Keywords: Syndiotactic polypropylene; Elasticity; Rheo-optical FTIR dichroism

1. Introduction and background

The physical properties of semicrystalline polymers depend strongly on crystalline structure and chain conformation. This dependence is especially evident in syndiotactic polypropylene (sPP) since it exhibits many different polymorphs and chain conformations. Recent advances in metallocene catalyst chemistry have made it possible to control the tacticity of polymers [1]. Variations in tacticity have profound effects on thermal and physical properties. This is especially true for sPP, which has a rich variety of crystalline morphologies [2–14].

Four different crystalline morphs have been identified for syndiotactic polypropylene. Forms I and II, are composed of macromolecular chains in s(2/1)2 helical conformation $(ttgg)_n$ and packed into orthorhombic unit cells. The crystalline Forms III and IV are composed of chains possessing *trans*-planar $(tttt)_n$ and $(t_6g_2t_2g_2)_n$ conformations, respectively. Form I is the most thermodynamically stable form [4,5]. The two fold helical chains are packed antichirally with alternation of right-and left-handed helices along both axes of the unit cell. Ideal form I is obtained by crystallization of highly stereoregular sPP at high temperatures (> 120 °C), occupying an orthorhombic unit cell with cell parameters being $a = 14.5$ Å, $b = 11.2$ Å and $c = 7.45$ Å (space group *Ibca*)[6,7]. At lower temperatures, form I still crystallizes but departs from fully antichiral packing due to kinetic reasons and defects that are introduced into the chain packing [6,7]. Form II is obtained in annealed fiber samples of sPP that have been stretched and having formed form III [8]. It is also obtained by tensile drawing films of syndiotactic polypropylene, which have low stereoregular content [8,9]. The unit cell corresponds to a *c*-centered structure in which helical chains having the same chirality are packed adjacently along both the transverse axes. The unit cell parameters are $a = 14.5$ Å, $b = 5.6$ Å and $c = 7.45$ Å. Form III consists of *trans*-planar zigzag conformed chains packed in an orthorhombic unit cell of lattice parameters $a = 5.22$ Å, $b = 11.7$ Å, $c = 5.06$ Å [10,11]. Form

---

* Corresponding author. Tel.: +1 313 577 3879; fax: +1 313 577 3810.
E-mail address: rkannan@che.eng.wayne.edu (R.M. Kannan).

0032-3861/$ - see front matter © 2005 Elsevier Ltd. All rights reserved.
doi:10.1016/j.polymer.2005.05.144

III has been obtained by drawing melt quenched, melt crystallized, and melt spun fibers to high tensile strains ($>400\%$) [12]. Form IV consists of chains in the $(t_6g_2t_2g_2)_n$ conformation, which is intermediate between the helical $(ttgg)_n$ and the *trans*-planar conformation [13,14]. It is obtained by the exposure of sPP fibers originally rich in form III to suitable solvent vapors at temperatures below 50 °C [14].

When a slow cooled, highly stereoregular sPP is deformed well beyond the yield point, it undergoes a transformation from form I that is composed of helical chains, to form III that is composed of *trans*-planar chains [15,16]. The process of transformation is one in which plastic deformation of the orthorhombic form I is accompanied by a change in the overall chain conformation from helical $(ttgg)_n$ to *trans*-planar $(tttt)_n$. Upon release of tension, there exists a reversible transformation from the *trans*-planar chain conformation back to the helical chain conformation [17]. The mesomorphic form is an intermediate crystallographic morph, which precedes the formation of form III during the process of stretching. This form also occurs upon release of tension. The elastic recovery is attributed to two possible influences, the first being enthalpic, which is due to crystallographic form III transforming back to a helical form II or the mesomorphic form. The second is entropic, which is due to the presence of the *trans*-planar chain conformation, which reverts back to the thermodynamically stable helical form. This combination of enthalpic and entropic factors is believed to result in the elastomeric behavior of sPP at high strains [17].

Elasticity in highly syndiotactic polypropylene has been investigated over the past few years [12,17–19]. When sPP films are stretched at room temperature to high strains ($\gtrsim 500\%$), there is a formation of *trans*-planar form III crystals. A decrease in elastic recovery is obtained when the temperature is increased to 80 °C [17]. High temperature stretching has been performed at temperatures of 40, 60 and 80 °C. The stretching performed at temperatures of 60 and 80 °C indicate the presence of the helical conformation when stretched to strains of 600%. Upon release of tension the helical chains in form I polymorph still exists. A detailed investigation of these transformations at high temperatures, and their relation to the reduced elasticity is the objective of this paper. Stretching of sPP has also been performed at 4 °C on samples containing different amounts of the *trans*-planar mesomorphic form and helical crystalline form. Depending on the initial mixture of crystals the authors observed the formation of either form III or mesomorphic form when stretched. At higher strains ($>400\%$), the mesomorphic form transformed to form III. When the tension is released there is a transformation to a mixture of helical and *trans*-planar forms. The relative amount of helical and mesomorphic forms depends on the temperature of stretching. The elasticity in lower stereoregular sPP has also been studied. Upon stretching, form III is observed but in smaller quantities and it reverts back to form II or the mesomorphic form when released [18–20].

The transformation of stretched form III when released has been debated in the literature [9,12,17–19]. In quenched samples with helical form I crystals, the stretching produces *trans*-planar form III, and upon release the sample reverts to helical form I and partial amounts of *trans*-planar mesomorphic form. However, there is small possibility for the low energy mesomorphic form to revert back to the high-energy form I upon release of tension. A transformation to form II is, however, possible as described before.

The purpose of the present work is to understand the changes that occur in sPP during tensile deformation and subsequent recovery at different temperatures, by using rheo-optical FTIR spectroscopy and X-ray diffraction. FTIR spectra provide us information about the differences in chain conformation the polymer exhibits upon stretching to different strains. During the process of stretching the crystallites present in syndiotactic polypropylene undergo yielding, which allows a conformational change to occur from helical to *trans*-planar. The point at which the transformation occurs is monitored both at room temperature and at elevated temperatures. The air-cooled specimen is utilized in the present study, which differs from isothermally crystallized samples that are crystallized at a particular crystallization temperature (T_c). The use of the air-cooled sample allows us to carefully control the extent of the helical to *trans*-planar conformational change when stretched with an increase in temperature. By simultaneously measuring dichroism we can observe the relative orientation of the *trans*-planar and helical chain conformation, and gain insights into the path taken by the helical conformation as it gets transformed to *trans*-planar conformation. Under identical sample preparation conditions, the stretched sPP recovers to different extents at different temperatures. This process when studied with FTIR spectroscopy may provide a more complete understanding of the transformation from helical to *trans*-planar and its effect on the elasticity of sPP.

2. Experimental

2.1. Sample preparation

Highly syndiotactic polypropylene (~90% *rrrr*, $M_w = 228{,}500$ g/mol, $M_n = 60{,}600$ g/mol) was obtained from the Fina Oil and Chemical Company (Dallas, TX, USA). Triple detection GPC measurements revealed $M_w/M_n = 3.77$. sPP pellets are heated to 170 °C in a hot press (Hydraulic Unit model 3912, Carver Inc.) and allowed to melt thoroughly between steel plates ($T_m = 135$ °C). The melt is then pressed lightly, resulting in a thin film of nearly uniform thickness (200–250 μm). Upon releasing the load, the film temperature is maintained at 170 °C for 30 min. This annealing step allows any molecular orientation imposed by melt pressing to relax. After annealing, the films are removed from the press and allowed to cool under ambient conditions (at an approximate cooling rate of 25 °C/min). This sample preparation method favors the formation of semi crystalline sPP composed primarily of helical chains (most likely disordered form I). A distribution of crystal size is present in the air-cooled sample. This is unlike isothermal crystallization at a particular temperature (T_c), where the crystal size is more uniform. We believe that the presence of a distribution of crystal sizes may play an important role in the reduced elasticity observed at higher temperatures.

2.2. Mechanical testing

Rectangular gauge samples (10×6 mm^2) cut from bulk films are used for all experiments. Tensile stress–strain data are collected using a strain-controlled Miniature Materials Tester (Minimat 2000, Rheometric Scientific Inc.). Gauge films are stretched stepwise at an elongation rate of 1 mm/min to specific strain values up to a final strain of 200%. In stepwise stretching the film is stretched to a particular strain and held, after which the IR absorbance and dichroism spectra are collected. The stretching is resumed upon acquisition of spectrum to the next point of strain. IR absorbance and dichroism spectra are collected at each strain point, in situ. For elevated temperatures, the films are equilibrated for 30 min at the chosen temperature. To facilitate both isothermal conditions and optical transparency, a custom-modified environmental chamber with KBr windows is integrated with the tensile tester. After stretching, and rheo-FTIR measurements are made in situ, the films are unhooked and allowed to relax fully at room temperature. The amount of tensile recovery for each film is then measured manually with a graduated ruler.

2.3. Rheo-FTIR spectroscopy

The Infrared absorbance and linear dichroism spectra are collected for each sample film both while under tension (in situ), and while relaxed (ex situ). This is achieved using a custom-developed rheo-FTIR spectrometer [21,22], which combines broadband polarization photoelastic modulation (model PEM-90/ZS37, Hinds Instruments, Inc., Hillsboro, OR) and step-scan interferometry (model FTS 6000, Bio-Rad/Digilab, Randolph, MA) with rheometry in order to measure quantitative IR dichroism spectra directly and rapidly. For ex situ conditions (i.e. both prior to stretching and post-stretch), high-resolution absorbance spectra (4 cm^{-1} resolution, 4 scans co-added) are collected using rapid-scan (continuous-scan) interferometry. In situ absorbance spectra and all IRLD (infra red linear dichroism) spectra are collected in step-scan mode. Fewer scans are co-added at higher temperatures in an effort to observe the increasingly rapid orientation/relaxation response of sPP (2 scans at 50 °C, 1 scan at 70 °C). The time required to complete a scan ranges from 60 s at room temperature to 30 s at 50 °C and 15 s at 70 °C. Quantitative results are obtained by normalizing raw spectra with appropriate background spectra.

Static IRLD experiments, involve three different pairs of background spectra: aligned-polarizer ($P_B(\tilde{\nu})$ and $P_D(\tilde{\nu})$), crossed-polarizer ($Q_B(\tilde{\nu})$ and $Q_D(\tilde{\nu})$), and open-beam (M_B and M_D). Aligned polarizer spectra are acquired with a second polarizer (an 'ideal anisotropic' sample) placed between the PEM and the detector. Crossed polarizer spectra are obtained by rotating the second linear polarizer by 90°, so that its polarization axis is perpendicular to that of the first polarizer. Open beam spectra are acquired with the second polarizer removed from the IR beam path. $P_B(\tilde{\nu})$, $P_D(\tilde{\nu})$, $Q_B(\tilde{\nu})$ and $Q_D(\tilde{\nu})$ contain information about the polarization modulation efficiency of the PEM as well as residual anisotropy of the optical train. M_B and M_D contain information about the optical throughput of the instrument.

The subscript B refers to the double modulated detector signal, which is demodulated first by a lock in amplifier (referenced to the PEM), and then for the 400 Hz phase modulation of the step-scan spectrometer. The subscript D refers to the raw absorbance signal, which is obtained by demodulating the detector signal using 400 Hz reference signal only.

$\bar{V}_D(\tilde{\nu}, \varepsilon)$ is proportional to the static absorbance of the sample, whereas $\bar{V}_B(\tilde{\nu}, \varepsilon)$ is proportional to the static dichroism of the sample. These two spectra are recorded with each incremental increase in strain.

$T_\parallel$, $T_\perp$ are the parallel and perpendicular transmittances which are calculated using the equation.

$$T_\parallel(\tilde{\nu}, \varepsilon) = \frac{P_B(\tilde{\nu})V_D(\tilde{\nu}, \varepsilon) - P_D(\tilde{\nu})V_B(\tilde{\nu}, \varepsilon)}{P_B(\tilde{\nu})M_D(\tilde{\nu}) - P_D(\tilde{\nu})M_B(\tilde{\nu})},$$

$$T_\perp(\tilde{\nu}, \varepsilon) = \frac{Q_B(\tilde{\nu})V_D(\tilde{\nu}, \varepsilon) - Q_D(\tilde{\nu})V_B(\tilde{\nu}, \varepsilon)}{Q_B(\tilde{\nu})M_D(\tilde{\nu}) - Q_D(\tilde{\nu})M_B(\tilde{\nu})}$$

Absorbance is defined as the negative logarithm of transmittance. Thus, static IRLD spectra are expressed as

$$\Delta A(\tilde{\nu}, \varepsilon) = -\log\left[\frac{T_\parallel(\tilde{\nu}, \varepsilon)}{T_\perp(\tilde{\nu}, \varepsilon)}\right]$$

2.4. Wide-angle X-ray diffraction (WAXD)

WAXD experiments are performed using a Rigaku RU2000 rotating anode powder diffractometer. It is equipped with a copper target drum, a secondary beam graphite monochromator, and a scintillation counter detector. Diffractograms are generated using a tube acceleration voltage of 40 kV and a tube current of 150 mA. These operating parameters generate the characteristic Cu Kα_1 line ($\lambda = 1.54056$ Å). Using Datascan software, intensity vs. Bragg angle plots are acquired from $2\theta = 10$ to 30° at a rate of 0.6°/min and a step size of 0.03°. Quantitative analysis is then performed using the Jade software package. Relaxed sample films are affixed to an aluminium mount using adhesive tape. All WAXD scans are performed at room temperature.

3. Results and discussion

3.1. Tensile testing

The crystalline morphology of an air-cooled specimen of sPP consists of form I orthorhombic crystallites [5–7]. The crystallites deviate kinetically from ideal form I due to the fast cooling rates employed to prepare the sample. The chain conformation consists of helical $(\mathrm{ttgg})_n$ and amorphous chains. The engineering stress–strain curves for air-cooled sPP films stretched to 200% strain are shown in the Fig. 1(a). The films are stretched at different temperatures ranging from 25 to 70 °C at intervals of 10 °C. We observe a decrease in tensile strength of the film with an increase in temperature. The yield strength (UTS) decreases from 12.1 MPa at 25 °C to 8.3 MPa at 70 °C. The gradual decrease in strength is attributed to the softening the material undergoes with an increase in temperature. The difference between the points (1) and (2) which are indicated in the Fig. 1(a) for different temperatures is plotted in the Fig. 1(b). (The points marked (1) and (2) represent the UTS and the point of steady stress, respectively). We observe a decrease in this difference as the temperature increases. This difference in stresses, and its temperature dependence correlates with the extent of helical to *trans*-planar conformation change after plastic deformation. These results will be correlated using rheo-FTIR spectroscopy.

Fig. 1(c) represents the temperature dependence of the elastic recovery of the film after being stretched to 200%. The elastic recovery has been calculated from

$$\frac{\text{Length}(200\%) - \text{Length}(\text{after recovery})}{\text{Length}(200\%)} \times 100\%$$

Upon release of tension the sPP loses part of its strain to which it has been stretched. The decrease depends upon the temperature to which it has been stretched with smaller amounts of recovery losses at a higher temperature. There appears to be a strong correlation between the decrease in elasticity at elevated temperatures, and the decrease in the stress difference between the yield point and the region of steady stress. This will be coupled with IR absorbance measurements, to better understand the nature of the structure-structure transformation at elevated temperatures.

3.2. WAXD

X-ray diffractograms for stretched and relaxed sPP films at different temperatures are given in Fig. 2. As stretching temperature increases, relaxed films appear to possess greater amounts of helical chains relative to *trans*-planar chains. This is observed at $2\theta = 12.37°$, which corresponds to the (200) plane of forms I and II crystals (Table 2). The intensity of this peak increases steadily with increasing stretching temperature. Similar behavior is observed at the corresponding second-order peak ($2\theta = 24.92° \rightarrow$ forms I and II, (400) planes). The broad peak located at $2\theta = 16$–$18°$ shows a gradual 'shift' in position of its maximum—from greater to lesser Bragg angles—as stretching temperature increases. The (020) and (110) planes of *trans*-planar mesomorphic form give rise to diffraction peaks at $2\theta \approx 17°$. As temperature increases, there is a relative decrease in intensity at this peak and a corresponding increase at $2\theta \approx 16°$. The latter peak is assigned to the (010) planes of disordered form I.

Considering the rich morphology possessed by sPP, care must be taken during WAXD peak assignment. It is possible for two other crystalline morphs, forms III and II, to contribute to peak intensity at $2\theta \approx 16°$ and $2\theta \approx 17°$, respectively. This possible variance in peak assignment has been addressed with rigor in a previous work involving tensile-deformed sPP, and thus, only a brief discussion regarding assignment of the aforementioned peaks will follow [23]. The (020) planes of form III give a WAXD peak near $2\theta \approx 16°$ ($2\theta = 15.849°$, $d = 5.59$ Å). However, we are confident that form III is absent, simply because its characteristic peaks at other Bragg angles are all absent. Furthermore, we know that form III is not likely to be produced under the experimental conditions discussed (e.g. slow cooling from the melt, tensile stretching only to 200% strain, elevated temperatures while stretching). Another possible influence on the peak at $2\theta \approx 17°$ are the (110) peaks of form II. However, it is unlikely that form II contributes strongly to this peak for two reasons. First, the sample is highly stereoregular. De Rosa et al. have found that form II appears most readily in deformed films and fibers of less syndiotactic sPP [8,9,12,17]. Second, if form II were present (most notably, in the film stretched at 25 °C), the peaks at $2\theta = 12.37°$ and $2\theta = 24.92°$, as well as helical crystalline IR absorbance peaks (at $\nu = 812$, 867, 900, and 1005 cm^{-1}), would be greater in magnitude relative to corresponding mesomorphic peaks. Therefore, WAXD results indicate the weak signature of form II but complete absence of form III. These results will be correlated with FTIR spectroscopy.

3.3. Infrared absorbance spectra

FTIR absorbance spectra of unreformed, as prepared air-cooled sPP are shown in the Fig. 3(a). The morphology of the specimen has been described in the previous section. The spectrum shows the presence of the helical conformation. The peaks present at 812, 867, 977 and 1005 cm^{-1} are associated with the helical conformation (Table 1 and 2). The peaks 829, 963, 1130 cm^{-1}, which are representative of the *trans*-planar chain conformation, are completely absent in the air-cooled specimen. A single spectra of the air cooled

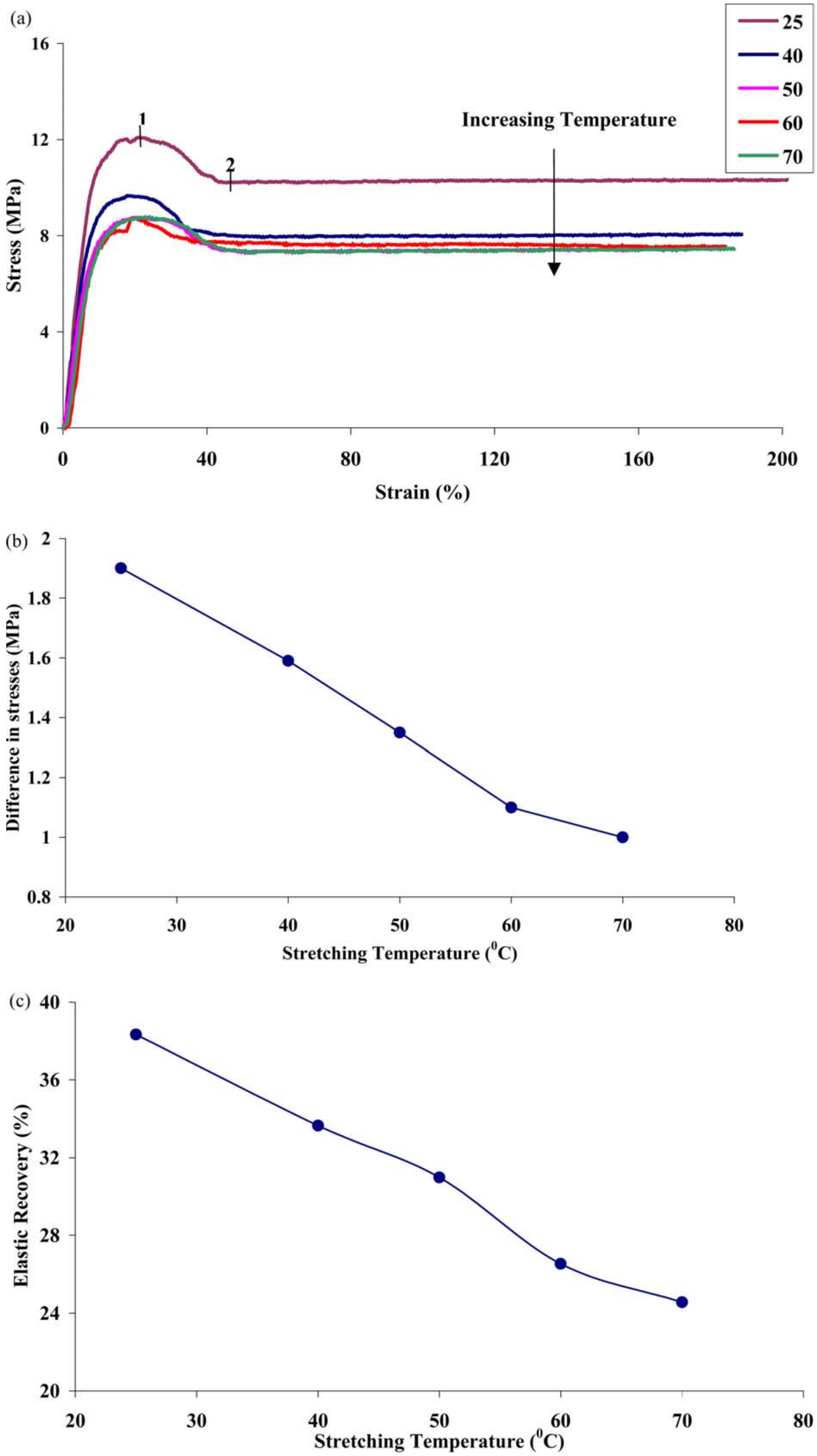

Fig. 1. (a) Tensile mechanical behavior of syndiotactic polypropylene films at different temperatures. The films are air cooled with a cooling rate of 25 °C/min. Test is performed at an elongation rate of 1 mm/min to a final strain of approximately 200%. (b) Difference in stress between the ultimate tensile strength (UTS) and point of steady stress for different stretching temperatures. (c) Elastic recovery (%) of syndiotactic polypropylene at different temperatures. Recovery has been calculated using the formula given in Section 3.

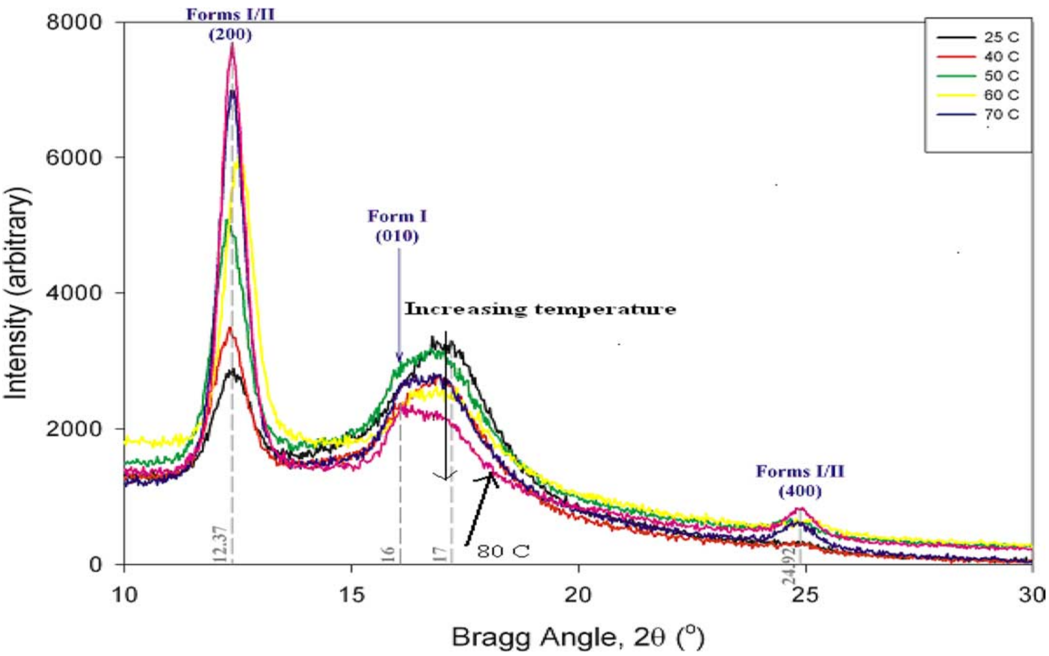

Fig. 2. Ex situ WAXD diffractograms of relaxed sPP films that have been tensile stretched to 200% strain at different temperatures.

Table 1
Conformation-sensitive infrared absorbance peaks for syndiotactic polypropylene

Wavenumber (cm^{-1})	Conformation assignment	Morphology assignment
812	Helical	Form I
838	Helical and planar (825 + 843 contributions)	Amorphous
867	Helical	Form I
963	Planar	Mesomorphic form and amorphous
977	Helical	Amorphous
1005	Helical	Form I
1131	Planar	Amorphous
1153	Conformation insensitive	Amorphous
1232	Planar	Amorphous

For each peak wavenumber are listed any molecular chain conformations or crystalline structures represented by the peak.

specimen is presented. This spectrum represents the conformation of the specimen tested both at room and at higher temperatures.

In order to elucidate the temperature and strain effect, we will discuss the static strain spectra at 50% strain at different temperatures in Fig. 3(b) and at a strain of 200% in Fig. 3(c). Fig. 3(b) represents the spectra of the air-cooled specimen stretched to 50% strain (just after yielding and corresponding to point 2 in Fig. 1(a)). Different spectra are a representation of different temperatures. The spectrum at room temperature suggests a conformational change from helical to *trans*-planar. The change in conformation is observed by the reduction in intensity of the helical peaks, which have been marked in Fig. 3(a), and the appearance of peaks indicative of *trans*-planar conformation (829, 963 and 1130 cm^{-1}). The point just beyond the yield at a strain of 50% represents the degree of conversion from helical to *trans*-planar. As the stretching temperature is increased we observe a decrease in the *trans*-planar content and a corresponding increase in the helical content at this particular point.

Table 2
Crystallographic parameters for sPP polymorphs

Polymorph	*hkl*	Observed $2\theta_{hkl}$ (°)
Helical (forms I and II)	200[a]	12.37
	020[b]/010[c]	~16
	400[a]	24.92

Bragg angles given are for Cu $K\alpha_1$ X-rays ($\lambda = 1.54056$ Å). Interplanar spacings, *d*, are also given for each *hkl* Miller indexed plane.

[a] Reflection is common to both forms I and II.

[b] Reflection is indexed based on limit-ordered form I ($b = 11.2$ Å).

[c] Reflection is indexed based on disordered form I ($b = 5.6$ Å).

The Fig. 3(c) represents the static spectra of the sample, which is further stretched to a strain of 200%. At room temperature we observe a further decrease in helical content accompanied by an increase in *trans*-planar content. Comparing the Fig. 3(a) and (b) we observe that the maximum amount of transformation occurs between points (1) and (2) in Fig. 1(a) and the transformation proceeds

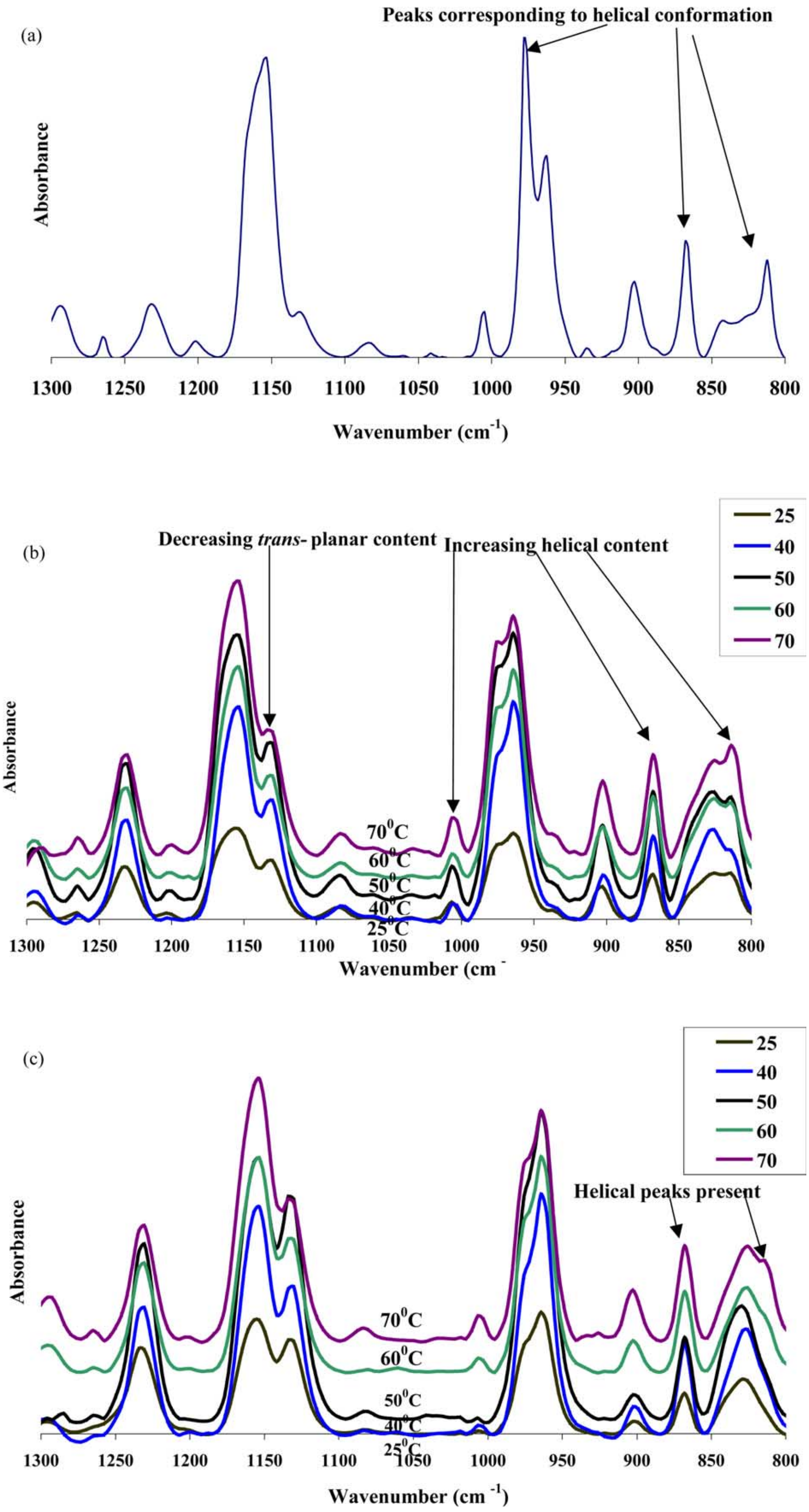

Fig. 3. (a) Step scan absorbance spectra of air-cooled syndiotactic polypropylene. Helical peaks are present at 812, 867 and 1005 cm^{-1}. Absence of *trans*-planar peaks at 839, 1131 cm^{-1}. (b) Step scan absorbance spectra of syndiotactic polypropylene at 50% strain for different temperatures. Non-transformed helical peaks are present at higher temperatures with decreasing amount of *trans*-planar content at higher temperatures. (c) Step scan absorbance spectra of syndiotactic polypropylene at 200% for different temperatures. Non-transformed helical peaks are present with increasing temperatures.

towards near completion at a strain of 200%. This is observed in Fig. 3(c). With an increase in temperature an increase in helical content is observed at the expense of decreasing *trans*-planar content. The helical peak at 812 cm^{-1} is present at room temperature and increases as the temperature is increased. Thus, at room temperature relatively low amount of the helical content is present at 200% strain, and the helical content increases with an increase in temperature due to the incomplete conformational change occurring at the yield point. In contrast, the *trans*-planar peak present at 1130 cm^{-1} is found to decrease with an increase in temperature.

3.4. Temperature dependence of elasticity

Fig. 4 represents the absorbance spectrum of sPP when released from a strain of 200% at different temperatures. We observe an increase in the helical peaks present at 812, 867 and 1005 cm^{-1} as compared to similar peaks at 200% strain in Fig. 3(c). There is a corresponding decrease in the *trans*-planar chain content. This is indicated by a decrease in magnitude of the peaks present at 829, 963 and 1130 cm^{-1}. Our results suggest that there exists a reversible conformational change from helical to *trans*-planar and back to helical when sPP is stretched and released, in accordance with literature [12,17–19]. This plays a key role in the deformation-induced elasticity in sPP. This is accompanied by a crystallographic transition from form III back to form II or the mesomorphic form in the relaxed state [17–19]. Monitoring the crystallographic transition is beyond the scope of this work.

Previous work suggests that the origin of elasticity to be a reversible conformational change from form III in the stretched state to form II in the relaxed state. This crystal-crystal transformation is found to be martensitic. At temperatures of 60 and 80 °C it is observed that the transformation does not occur, which is the reason for reduced elasticity. Also form I is observed in the relaxed specimen at 60 and 80 °C [17].

A combination of crystal structure and chain conformation changes plays an important role on the elasticity in sPP. The air-cooled specimen used in the present study has different amount of form I crystals of different sizes when cooled from the melting point. The size of the crystal depends upon the temperature at which nucleation and crystal growth occur. In an air-cooled sample a distribution of crystal sizes is present. This is due to the different temperatures through which the sample passes during the process of cooling from above the melting point to room temperature. Each particular crystallite possesses a critical stress (σ_{cr}), which is dependent on the surface energy and the size of the crystal. Since, the specimen is air-cooled, different crystals are formed when the specimen is cooled from its melting point. The critical stress required is different for different crystallites possessing form I morphology. The critical stress (σ_{cr}) is the amount of stress required to cause dislocation and slip of form I crystals prior to yielding and could be different from σ_{cr} mentioned in literature [18,19], which is the critical stress required to cause transformation from forms II to III during cyclic stress strain. The deformation of a large portion of the crystallites occurs at room temperature since the critical stress is attained for all crystallites [24]. The deformed form I crystallites transform to the mesomorphic form, which forms an intermediate crystal structure prior to its transformation to form III. As the temperature is increased thermal softening of the material occurs. Portions of the form I crystallites do not attain the critical stress required for deformation. This portion of undeformed crystallites increases with an increase in temperature. The undeformed

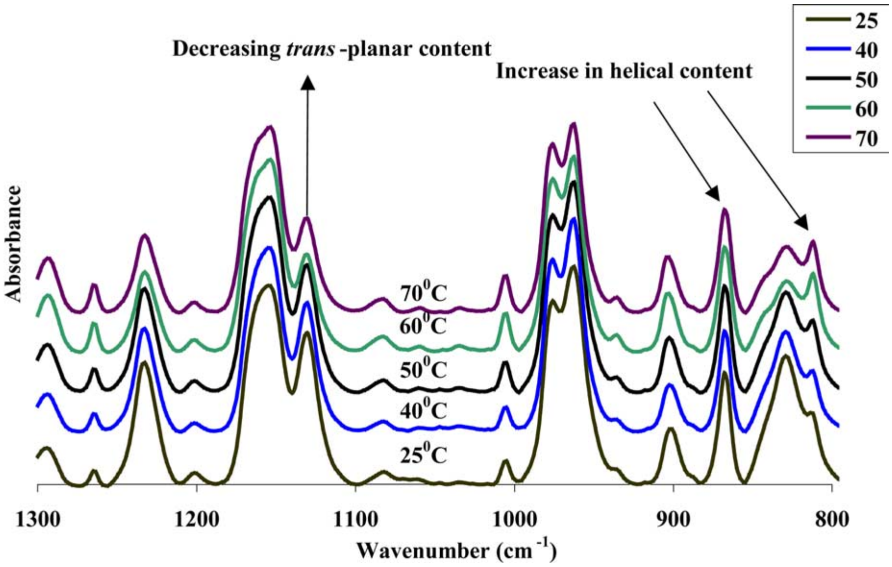

Fig. 4. Step scan spectra of sPP upon elastic recovery from a strain of 200%. The helical peaks present at 812, 867 and 1005 cm^{-1} increase in content as compared to Fig. 3(c) and a corresponding decrease in *trans*-planar content is observed.

crystallites do not allow the transformation from helical to *trans*-planar to occur and are present as form I beyond the yield point. Beyond the yield point, there could be near complete transformation from helical to *trans*-planar occurring at room temperature. On the other hand, such a transformation could be occurring to a lesser extent at 70 °C due to the critical stress (σ_{cr}) not being attained for the crystallites. This difference in chain conformation is present beyond the yield point between room temperature and higher temperatures at a strain of 50%, and persists when the specimen is further stretched to a strain of 200%. The reduced helical to *trans*-planar transformation also correlates with the reduction in the stress difference suggesting that is related to structure transformation (Fig. 1(b)).

When the strain is removed, the sample shows appreciable amounts of recovery at room temperature, with decreasing recovery as the temperature is increased. The *trans*-planar conformation, which appears beyond the yield point, plays a key role in the elasticity. It is present in greater amounts at room temperature and in smaller amounts at higher temperatures, and this correlates well with reduced elasticity. At room temperature and a strain of 200% *trans*-planar chains are present due to almost complete transformation. The specimen when released from 200% strain reverts back to the helical conformation. Upon increase of temperature the amount of transformation from helical to *trans*-planar decreases. At 70 °C (at 200%), there is a high proportion of helical chains (form I crystallites) and extremely small amounts of *trans*-planar chains (form III). Now, only the *trans*-planar chains participate in the recovery process (thus contributing to elasticity) while the helical chains do not participate in the process of recovery. At room temperatures, the relaxed specimen shows the presence of the helical conformation due to the transformation from *trans*-planar back to helical. As the temperature is increased the relaxed specimen contains a mixture of more helical and less *trans*-planar chains. This increase in helical signature is due to the combination of untransformed helical chains (form I) and the reversibly transformed helical chains (form II). The *trans*-planar chain content correspondingly decreases as the helical chain content increases.

3.5. Rheo-FTIR dichroism response

Rheo-optical FTIR dichroism provides an understanding of the extent of orientation in helical and *trans*-planar chains, during stretching. The stretching is performed at 25, 50 and 70 °C. Fig. 5(a) represents the linear dichroic (IRLD) spectra (for 0 to 200% strain) for air-cooled sPP at room temperature. These spectra should be interpreted in conjunction with the corresponding absorbance spectra, since, it provides insights into the relative helical and *trans*-planar content. The dichroism peak at 0% strain represents a small amount of residual orientation present during preparation of the sPP specimen. As the strain is increased to the yield point (∼30%) form I crystals increase in dichroism (812, 867 and 1005 cm^{-1} increase in magnitude). Upon yielding ($\varepsilon > 30\%$) the dichroism spectrum undergoes marked changes. The dichroism associated with helical peaks decrease in magnitude while the magnitude of *trans*-planar peaks increase in dichroism. The dichroism associated with amorphous chains also increases. Some peaks undergo a ‘flip’, which represents a change in the overall orientation direction of a given moiety [23,24]. This has been observed in deformation models representative of semi crystalline polymers. The decrease in dichroism of the helical peaks is due to a sharp decrease in the helical chain content upon yielding, which has been described in the IR absorbance section. Upon yielding, the dichroism of *trans*-planar peaks (829, 963 and 1130 cm^{-1}) increases in magnitude going from a strain of 50–200%, again due to the increase in *trans*-planar content.

At 50 °C there is an increase in dichroism compared to that at room temperature (Fig. 5(b)). This is due to the additional mobility the chains possess at higher temperature. At 25% strain, the trend in dichroic behavior is similar to that at room temperature i.e. the helical conformations represented by the wave numbers 812, 867 and 1005 cm^{-1} exhibit strong dichroism. Beyond the yield point there is a sudden increase in the dichroism of the *trans*-planar chains. The increase is greater in magnitude as compared to the increase dichroism associated with the helical chains. The sudden increase is accompanied by a change in sign of the dichroism of helical chains. The dichroism present is due to the initial high amount of helical content, and does not increase beyond the yield point. The extent of conformational change from helical to *trans*-planar is small at 50 °C as explained in the infrared absorbance section. Thus, we are able to distinguish between dichroism due to the mobility of the chains and dichroism that occurs due to the presence of a large amount of the particular conformation. The *trans*-planar conformation exhibits increased dichroism with increasing strains of 100, 150 and 200%.

At a higher temperature of 70 °C there is a higher helical content due to a smaller amount of transformation from helical to *trans*-planar that occurs upon yielding. (Fig. 5(c)). The dichroism of the helical peaks beyond the yield point is of a greater magnitude than at 25 or at 50 °C. The presence of a greater amount of helical chain content at higher temperatures, as has been explained in previous sections, results in higher dichroism.

A comparison of the dichroic deformation spectra at 25, 50 and 70 °C represent certain distinct differences. At 25 °C, we observe the largest dichroism to be of the 1130 cm^{-1} peak. The dichroism at 829 and 963 cm^{-1} is much smaller. At 50 °C, the 963 cm^{-1} peak shows the largest dichroism with a lower dichroism indicated by the 1130 cm^{-1} peak. This can be attributed to the faster relaxation during the measurement of the 1130 cm^{-1} dipole as compared to the 963 and 829 cm^{-1} dipoles. The 1130 cm^{-1} dipole may represent the amorphous portion of the *trans*-planar

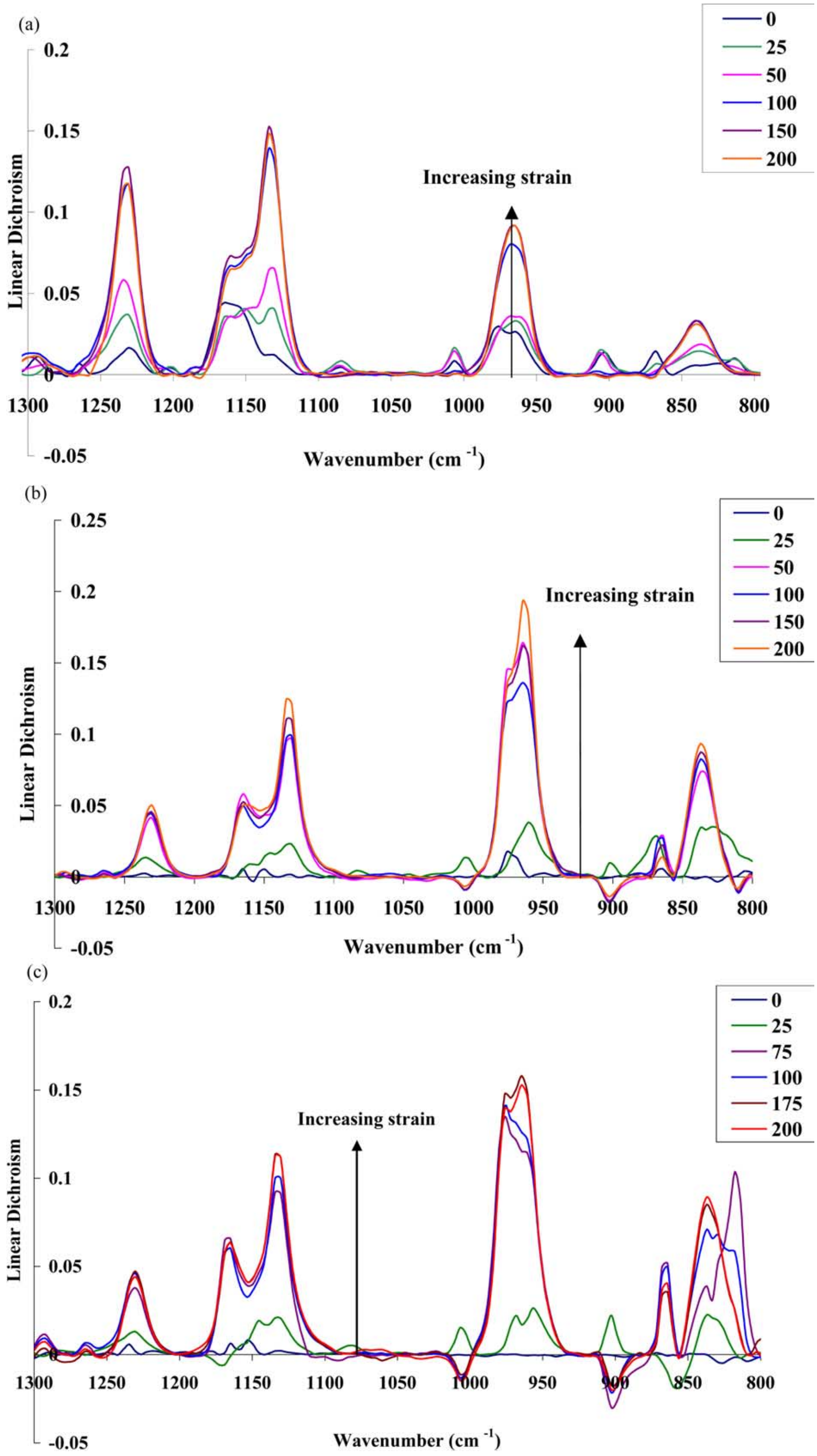

Fig. 5. (a) In situ IRLD spectra for air-cooled sPP tensile deformed to different strains at room temperature. Spectra are acquired in step scan mode with a resolution of 8 and 4 cm^{-1} scans co added. (b) In situ IRLD spectra for air-cooled sPP tensile deformed to different strains at 50 °C. Spectra are acquired in step scan mode with a resolution of 8 cm^{-1} and two scans co-added. (c) In situ IRLD spectra for air-cooled sPP tensile deformed to different strains at 70 °C. Spectra are acquired in step scan mode with a resolution of 8 cm^{-1} and one scan co added.

conformation. The *trans*-planar amorphous chains may relax at a faster rate than the 'more ordered' 963 or 829 cm^{-1} *trans*-planar dipoles. A decrease in dichroism is thus observed with an increase in temperature and a similar trend is observed at 70 °C.

The increase in dichroism of the *trans*-planar peaks observed beyond the yield point gives us an idea of the 'freedom' possessed by the *trans*-planar conformation. At 25 °C, the difference in dichroism between 25 and 50% strain of the 963 cm^{-1} peak is 0.055 but at a temperature of 50 °C the difference is 0.9 (Fig. 5(a)). A similar increase in the difference between room temperature dichroism and that at 50 °C is observed in the peak at 1130 cm^{-1}. This indicates the high degree of 'freedom' possessed by the *trans*-planar peaks at 50 °C. The crystallites prevent the orientation of the helical conformation prior to the yield point. However, upon deformation of the crystallites the conformational change occurs which gives extra 'freedom' to the *trans*-planar chains. This increase in entropy manifests itself as higher dichroism beyond the yield point.

The elasticity in sPP, as mentioned previously has been attributed to the reversible transformation from *trans*-planar back to helical. The non-transformed helices present at higher temperatures of 50 and 70 °C, do not orient in a manner that is similar to the *trans*-planar conformation. The helical peaks show only a small increase in dichroism after the yield point with increasing strain. This is in contrast to the *trans*-planar peaks, which exhibit a gradual increase in dichroism with increasing strain.

4. Conclusions

By performing WAXD and rheo-FTIR measurements we have monitored the helical to *trans*-planar conformational change in sPP at different temperatures. A decrease in elasticity (beyond the yield point) with an increase in temperature has been observed. This correlates with a reduced level of helical to *trans*-planar conformational change with an increase in temperature. FTIR provides 'quantitative' insights into the relative changes in the helical and trans-planar content. The *trans*-planar conformation plays a key role in the elasticity and decreasing amounts of this conformation results in lower elasticity levels. The stress difference between the yield strength and the point of steady stress also correlate with the extent of helical and *trans*-planar conformational change.

X-ray diffraction is also utilized to further examine the relaxed sPP. Upon relaxation, the form II morph or the mesomorphic form appears. This corresponds well with literature, which indicates the reversible transformation from form III (upon stretching $>400\%$) to either form II or the mesomorphic form. The X-ray results confirm in part and agree with literature about the origins of elasticity in sPP. Reasons for elasticity in highly syndiotactic polypropylene have been observed in the literature to be two-fold. The enthalpic contribution comes from the crystal–crystal transformation which occurs when form I transforms to form III (upon stretching to strains greater than 400%) and then the form III reverting back to either the mesomorphic form or form II upon release of strain [18,19]. The entropic contribution comes from the change in conformation, which occurs when the helices transform to *trans*-planar conformation and then a portion of the *trans*-planar chains reverts back to the helical conformation [18,19].

The present work clarifies the reasons for reduced elasticity at higher temperatures using an air-cooled specimen. The decreased elasticity and recovery is due to a decrease in the amount of transformation at the point of yield. Thus at higher temperatures the untransformed helical chains (form I) remain beyond the yield point due to the critical stress not being attained. The untransformed helical chains are present at 200% strain. When the specimen is released at strains of 200% the helical chains belonging to form I do not participate in the process of recovery. This results in only the *trans*-planar chains of form III reverting back to the helical chains of form II. This explanation differs from Ref. [17], where annealing brings about the presence of form I.

Rheo-optical FTIR studies provides further insights into the elasticity in syndiotactic polypropylene. Different proportions of helical and *trans*-planar conformations orient to different extents. The helical conformation does not orient at a higher temperature though they are present beyond the yield point. In contrast, the *trans*-planar chains show a significant increase in dichroism beyond the yield point, suggesting that there is a difference in mobility (orientation) of the helical and *trans*-planar chains. This further supports the importance of *trans*-planar chains on the elastic behavior. The dichroic spectra also allow us to distinguish the responses from *trans*-planar chains in the amorphous, and those in the mesomorphic form. The model for deformation in semi crystalline polymers can further be understood by tracking chain mobility. The *trans*-planar conformation gains in entropy upon crystal deformation. This is shown as an increase in dichroism.

Acknowledgement

We thank Dr Gulay Serhatkulu in helping us with the powder diffraction measurements. We thank the Fina Oil and Chemical company LaPorte, TX for providing us with the sPP samples. Financial support from NSF DMR 9876221 and WSU (IMR) are gratefully acknowledged.

References

[1] Ewen JA, Jones RL, Razavi A. J Am Chem Soc 1988;110:6255–6.

[2] Sevegney M, Kannan RM, Siedle AR, Percha P. J Polym Sci (PP) 2004;43(4):439–61.

[3] Sevegney M, Kannan RM, Naik R, Naik V. FTIR spectroscopic investigation of thermal effects in semi-syndiotactic PP. Accepted for Publication in Vibrational Spectroscopy, 2005.

[4] Lotz B, Lovinger AJ, Cais RE. Macromolecules 1988;21:2375–82.

[5] Lovinger AJ, Lotz B, Davis DD. Polymer 1990;31:2253–9.

[6] Lovinger AJ, Lotz B, Davis DD, Padden Jr FJ. Macromolecules 1993; 26:3494–503.

[7] Lovinger AJ, Davis DD, Lotz B. Macromolecules 1991;24:552–60.

[8] De Rosa C, Corradini P. Macromolecules 1993;26:5711–8.

[9] De Rosa C, Auriemma F, Vinti V. Macromolecules 1998;31:7430–5.

[10] Natta G, Corradini P, Ganis P. Makromol Chem 1964;75:215–6.

[11] Natta G, Peraldo M, Allegra G. Makromol Chem 1964;39:238–42.

[12] Auriemma F, Ruiz de Ballesteros O, De Rosa C. Macromolecules 2001;34:4485–91.

[13] Chatani Y, Maruyama H, Asanuma T, Shiomura T. J Polym Sci, Polym Phys Ed 1991;29:1649.

[14] Auriemma F, De Rosa C, Ruiz De Ballesteros O, Vinti V, Corradini PJ. J Polym Sci, Polym Phys 1998;36:395–402.

[15] Guadagno L, D'Aniello C, Naddeo C, Vittoria V, Meille SV. Macromolecules 2002;35:3921–7.

[16] Loos J, Schimanski T. Polym Eng Sci 2000;40:567–72.

[17] De Rosa C, Gargiulo MC, Auriemma F, Ruiz de Ballesteros O, Razavi A. Macromolecules 2002;35:9083–95.

[18] Auriemma F, De Rosa C. J Am Chem Soc 2003;125:13143–7.

[19] Auriemma F, De Rosa C. Macromolecules 2003;36:9396–410.

[20] De Rosa C, Ruiz de Ballesteros O, Auriemma F. Macromolecules 2004;37:7724–35.

[21] Hofmann GR, Sevegney MS, Kannan RM. Int J Poly Anal and Char 2004;9(4):245.

[22] Noda I, Dowrey AE, Marcott C. A spectrometer for measuring time-resolved infrared linear dichroism induced by a small-amplitude oscillatory strain. Appl Spectrosc 1988;42:203–16.

[23] Sevegney MS, Parthasarathy G, Kannan RM, Thurman DW, Ballester LF. Macromoecules 2003;36:6472–83.

[24] Loos J, Petermann J, Waldofner A. Colloid Polym Sci 1997;275(11): 1088–92.